Controlled spray quenching in heat treatment process

B. Hinrichs[1], N. Hornig, S. Schüttenberg, U. Fritsching
Process & Chemical Engineering, Foundation Institute for Materials Science (IWT),
Badgasteiner Str. 3, Bremen, Germany
b.hinrichs@iwt.uni-bremen.de and hornig@iwt.uni-bremen.de

Abstract

Spray quenching is a method for precise control of material and workpiece properties of metallic specimen in heat treatment processes. Specific material microstructure distributions in combination with the avoidance of workpiece distortion in heat treatment processes may be realized by impressing precisely controlled cooling with flexible flow fields based on multiple two phase spray nozzle arrangements.
This contribution describes the use of spray cooling techniques for specific quenching of simple shaped aluminum and steel specimen in heat treatment processes. For efficient estimation of the cooling process a spray characterization, consisting of drop velocity, drop diameter and impingement density measurements in combination with measurements of local heat transfer coefficients (HTC) is performed. The HTC-profile measurements were obtained from the solution of the inverse heat conduction problem based on thermographic temperature measurements during spray cooling of thin sheets. The results are validated with established calculation and model approaches and numerical cooling simulations.

Introduction

The heat treatment process of e.g. steel and aluminum is an important production step in metal working industries. The material performance can be increased in a high range by heat treatment. Controlling of the quenching process and optimizing the performance of the parts are the targets of intensive researches [1][2]. The advanced performance helps to build more complex and lighter parts in an economical way. The use of high performance workpiece reduces the need for energy and further resources in the production.

The heat treatment and therefore the quenching of metal parts is the main process to increase the performance of metal workpiece [3][4]. The performance of steel and aluminum alloys over the time temperature curve is shown in the time-temperature-transformation ttt- and iso-ttt-diagrams. For example within the cooling of steel, from the austenite into some other phases like bainite or ferrite, the microstructure cores start growing and changing their configuration. These phase changing and mixing processes are time-dependent and point out the main processes for the material performance, which are directly connected to the temperature change over the time. High performance parts need defined local properties to resist a locally applied load. For example gearwheels need hard tooth flanks to decrease the abrasion as well as a more ductile tooth base to decrease the impact load of contact. Therefore an intense quenching of the tooth flank should be applied as well as a lesser quenching intensity of the tooth base [4].

The industrial standards of quenching methods in heat treatment are gas quenching, spray quenching, jet quenching, and dipping bath quenching. These types of quenching have advantages and disadvantages through different levels of HTCs. The heat transfer coefficient ranges from 10 W/m^2K up to 1000 W/m^2K for gas quenching, from 600 W/m^2K to 42000 W/m^2K [5][6] for spray quenching and up to 2000 W/m^2K till 42000 W/m^2K for jet quenching [7]. High HTC gradients may lead to thermal stresses and distortion of the components. Depending on material, microstructure, ttt-diagrams, quality of distortion and amount of heat treated workpieces are to be designed.

Furthermore the necessary cooling rates are depending also on the geometric shape of the workpiece. In some cases, heavy parts with different wall thickness are used. These parts need high HTCs to reach the targets cooling rate inside but also need a variable cooling rate to avoid an undercooling of the surface. Time-depending cooling rates are needed to create a high performance microstructure in an exemplary shoulder shaft (figure 7). This is equal to aluminum parts, mostly profiles, casting or forging with variations in thickness, which also need fast quenching rates at thin sections and slow rates at thicker sections. The shouldered shaft represents a simplified gearing specimen, which is frequently used and produced in the industrial environment.

The spray quenching in controlled flexible spray fields combines the advantages of local defined wide ranged HTC leading to high strength and less distortion [4][8]. Controlled spray quenching in flexible fields avoid distortion in heat treatment processes by impinging the part with asymmetric and variable HTCs. In comparison to water dipping bath quenching, the disadvantage of the Leidenfrost phenomenon can be avoided by

1 Corresponding author: b.hinrichs@iwt.uni-bremen.de

sprays with lower amount of water [5]. The wetting of the workpiece can be controlled by the nozzle setup and the process parameters. Single droplet evaporation can be realized to avoid the development of a consistent liquid layer on the surface, which is characterized as the Leidenfrost phenomenon [9].

To create high performance parts with varying wall thicknesses, an asymmetric spray field with individual nozzle process parameter may be used. The process parameters for each nozzle are previously derived by numerical simulations and analytic dimensioning, to reach local-distributed quenching intensities [10]. This is followed by spray characterization (impingement density, drop size distribution, angle of spray, mean drop velocity distribution, mean gas flow velocity) determined by experimental investigations with patternator measurements (mass flux), laser diffraction spectrometry (drop size), particle image velocity (drop velocity) and quenching test (HTC and temperature) [4]. The resulting HTC is estimated according to the process parameters. These heat transfer coefficients are compared to results of other tests and implemented into numerical simulations of heat transfer for various parts. For representing a specimen during a quenching process, possessing surface areas of direct water impingement, predefined surfaces of the specimen model can be implemented by applying calculated heat transfer coefficients [11] through user defined functions (UDF). Numerical simulations help rating a quenching process in order to achieve a homogeneous temperature profile to reduce distortion.

Experimental determination of the heat transfer coefficient distribution in impinging sprays

The heat transfer coefficient measurements are divided into two main setups. The first setup is based on determining the surface temperature via infrared thermal imaging during spray quenching [12]. Figure 1 shows the schematic trials setup for the infrared measurements.

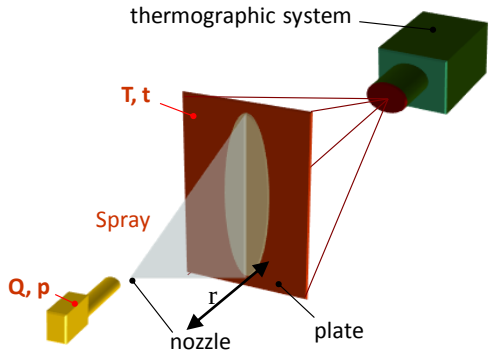

Figure 1 Schematic exposition of the infrared surface temperature measurement setup.

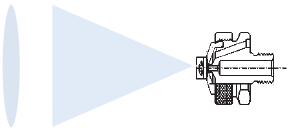

Figure 2 Two phase external mixing flat spray nozzle

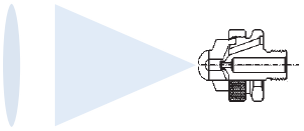

Figure 3 Two phase internal mixing flat spray nozzle

The setup is composed of a nozzle, a heated (thin) plate and a thermographic camera system. The used nozzle are flat spray two phase mixing nozzles with a liquid mass flow range from 0.05 l/min to 27 l/min, a gas pressure range of 1 bar to 6.3 bar and a spray angle of 90°. For comparison also internal (figure 3) and external (figure 2) mixing nozzles are used to validate the influences on the cooling behaviour. The used fluids are water as the liquid phase and air as the gas phase.

Different test plates are used for the thermographic, which are described in table 1. To determine the variation of the emission coefficient of the plate, the side facing the thermo camera, is coated with matt black lacquer to achieve an emission coefficient of $E \approx 0.9$.

assay	material	thickness	dimensions
1	steel	5 mm	ø = 200 mm
2	steel	3 mm	200 x 200 mm
3	aluminum	3 mm	200 x 200 mm

Table 1 Assay table with the different used geometries and materials

The different parts are used to determine the influence of different materials and probe geometries [13]**.** The camera system is a Vario CAM HiRes 640.

Initially the part is heated up in a box furnace to more than 550 °C for aluminum plates and 850 °C for steel plates. After achieving a homogenous temperature distribution in the plate, the plate is manually removed from

the oven and placed in the setup. The heat loss during this operation is approximately 50 – 70 °C in surface temperature. The quenching starts immediately the spray nozzle is positioned perpendicular onto the metal workpiece surface with a distance between nozzle and workpiece surface of r = 100 mm. The surface temperature is detected on the opposite position during the quenching via the thermographic system. The detection frame rate is 50 frames per second (fps) with a resolution of 640 x 480. Solving the inverse heat conduction process, the transient, quasi one dimensional heat conduction [4] process or the Lumped Capacitance Method (LCM) allows determination of the local and temporal heat transfer coefficient distribution from the surface temperature measurements.

The second setup is an industrial quenching process demonstration process setup. The controlled flexible spray field is an arrangement of eight nozzles evenly spread around the specimen divided into two segments. The nozzle position, distance and angle to the specimen surface are variable. Figure 4 shows the schematic arrangement for a quenching process of a shouldered shaft and figures 5, the used arrangement.

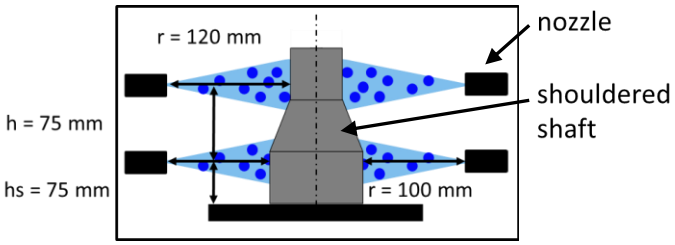

Figure 4 Schematic trials setup.

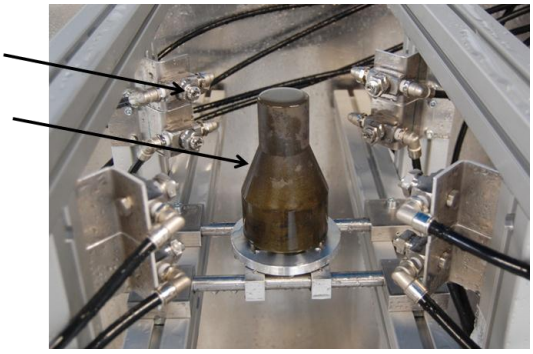

Figure 5 Arrangement of eight flat spray nozzles for flexible spray quenching of a shouldered shaft

The distance between the nozzles and the shaft surface is at least 100 mm. For minimal distortion and maximum process control, the gas pressure and the liquid mass flow rate can be controlled for each segment separately, whereby a large number of asymmetric quenching conditions can be applied. The actual experiments are performed with the shouldered shaft specimen shown in figure 6.

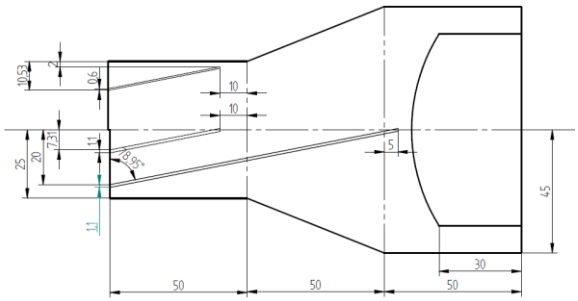

Figure 6 Quenching assembly shouldered shaft including drilling for thermocouples

The nozzles arrangement allows a certain overlapping in critical zones. Initially the heated shouldered shaft is manually transferred into the spray field. Immediately the quenching starts and the temperature distribution at certain points inside the specimen are recorded. The temperature is measured by thermocouples, type K, in certain drillings of the workpiece. One thermocouple is placed close to the surface (0.6 mm drilling), this thermocouple is facing the spray direction. This thermocouple detects a virtual surface temperature for evaluation of the HTC during the quenching process. The flexible arrangement and separate adjustment of process parameters, within the position of the nozzles, allows asymmetric quenching of different wall thicknesses, geometries and materials.

The cooling curves of the thermographic trials and of the flexible spray field trials are analyzed in the following chapters.

Results and Discussion

The process parameter show similar behaviour to the cooling rates as the literature findings [14][11][3]. Higher fluid volume flows increase the cooling rates of the specimen. In comparison to the fluid volume influence the gas pressure influence can be neglected for these trials, the influence is too small. Therefore the time-temperature boundary in transient measurements is considered in detail. Based on the time-temperature-functions the heat transfer coefficient distribution is determined. The approximation of the HTC is based on the transient heat conduction in a static body.

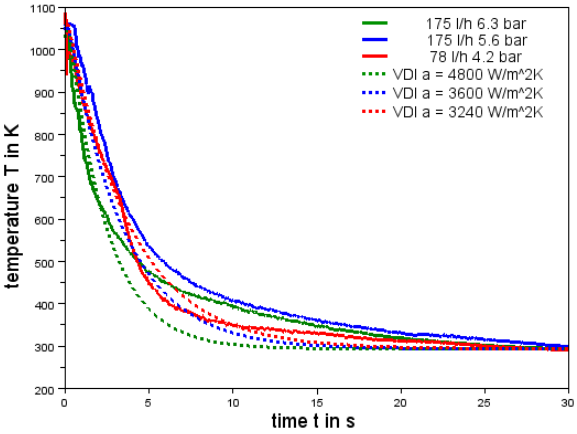

Figure 7 Exemplary comparisons between calculated transient heat conducting and measurements.

Figure 7 shows an exemplary comparison between the analytic results of transient heat conduction of a plate (steel, thickness 5 mm) with a constant heat transfer coefficient [5][15] and the results of the spray cooling thermographic measurements. Some cases are not matching the analytic calculate with the assumption of a constant heat transfer coefficient. Depending on the Leidenfrost effect there are at least two different HTC values necessary, as shown in figure 8.

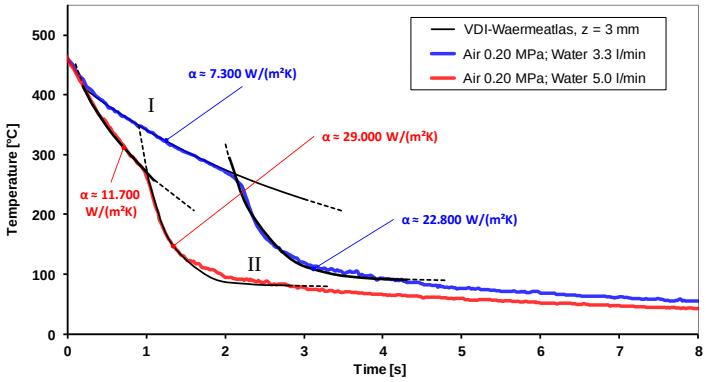

Figure 8 Exemplary comparisons between calculated transient heat conducting and measurements with two ranges

Furthermore the heat transfer in multiphase flow with phase changing (evaporating) fluids, here especially water, is strongly temperature dependent. The boiling curve in figure 9 shows the achieved temperature heat flux function versus surface temperature T_w, fluid temperature, saturation temperature T_{sat} of the fluid and heat flux q´´ or rather the heat transfer coefficient [15][16].

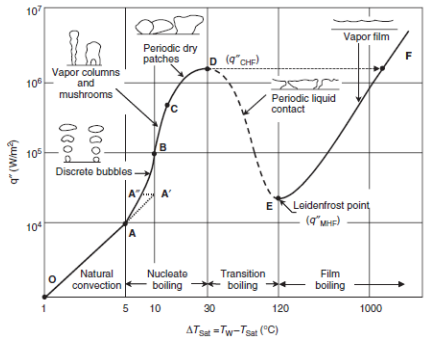

Figure 9 Boiling curve showing different regions in pool boiling [16]

For analysis of the connection between the surface temperature and the HTC a finite volume element with one surface side heat transfer mechanism is used to evaluate the time / temperature dependency of the heat transfer coefficient [12].
The energy balance, equation (1), gives information about the heat flux.

$$\rho c_p \frac{\partial T}{\partial t} = -\nabla \dot{q} \tag{1}$$

The heat flux is described by the HTC depending on the surrounding temperature, equation (2).

$$\dot{q} = \alpha(T_{sur} - T_{\infty}) \tag{2}$$

The time, temperature and material depending function of the HTC is derived.

$$\rho c_p \frac{\partial T_{sur}}{\partial t} = -\nabla\big(\alpha(T_{sur} - T_{\infty})\big) \tag{3}$$

The model, also used in [12][17], neglects the transient heat conduction in the specimen. Thermal energy transport may occur in surface normal (to the core) and tangential direction. The radial influence is a heat flux of the not impinged surface to the impinged. An analysis of a volume element in the middle of the spray cone minimizes the influence of the radial heat flux, with the priori statement of a homogeneous heat transfer coefficient in the center of the spray [3]. To derive the connection between temperature and HTC of sprays, the cooling curves are fitted with a grade 6 polynomial shown in figure 10.

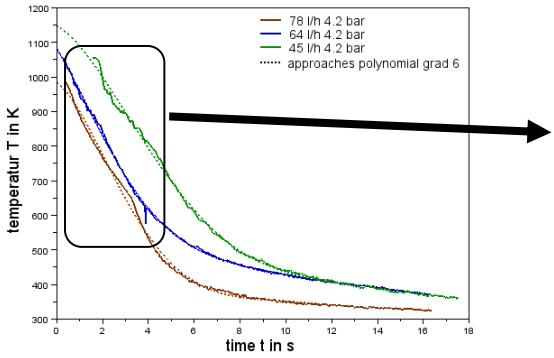

Figure 10 Approaches of cooling curves with a grad 6 polynomial

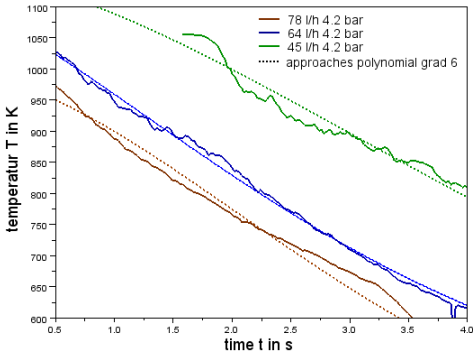

Figure 11 Failure of the approaching with smoothing of the cooling curves

The polynomial fitting shows the best approach to the measurement results [11]. By smoothing the time-temperature-function important points get lost, as figure 11 shows. The use of a single polynomial over the whole temperature range cannot match the unsteady cooling rate. Using more than one polynomial function for the whole range helps to image cooling curves and allows to approachs the time or rather the temperature depending HTC for a wide range and several points of interest, as shown in figure 12 und 13.

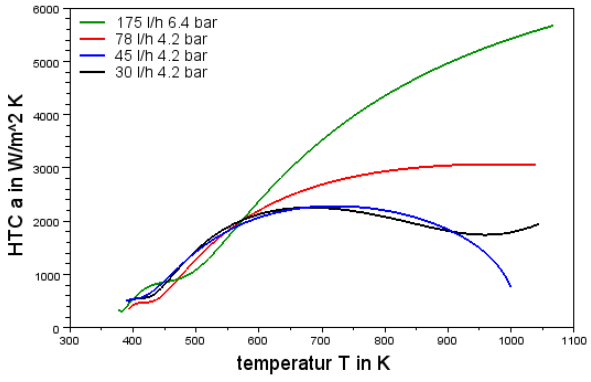

Figure 12 Exemplary diagram of the HTC / temperature curves for the wide range

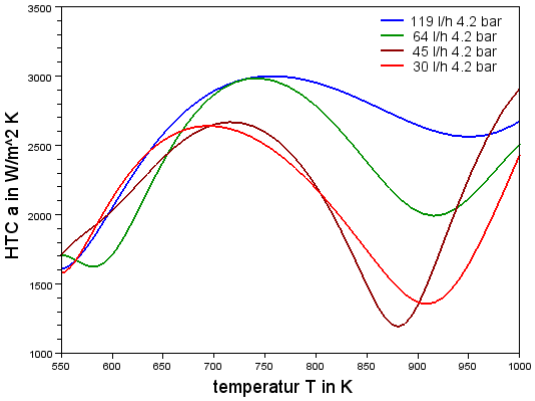

Figure 13 Exemplary diagram of the HTC / temperature curves for the range of 1000 K – 600 K

For lower temperatures the wide range HTC functions has a plateau at around 500 W/m^{2}K and increases at ≈ 450 K. Furthermore the HTC increases with a high rate at least until 600 K. A function between nozzle / process parameters and HTC / temperature curves is to be derived in analogy to e.g. [11][12]. Figure 13 is similar to figure 9 illustrating the function between HTC and temperature in principle agreement to the boiling curve. The spray impact moves the Leidenfrost point to higher temperatures and smooths the decreasing effect of the HTC. Combining the thermographic and the spray field results feature new technical expertise of the spray cooling. A thermographic image of the whole cooling area during the full time range carries the information of the temperature and the time for each pixel. A time versus temperature and a temperature–HTC run visualize the main spray area obtaining relevant information.

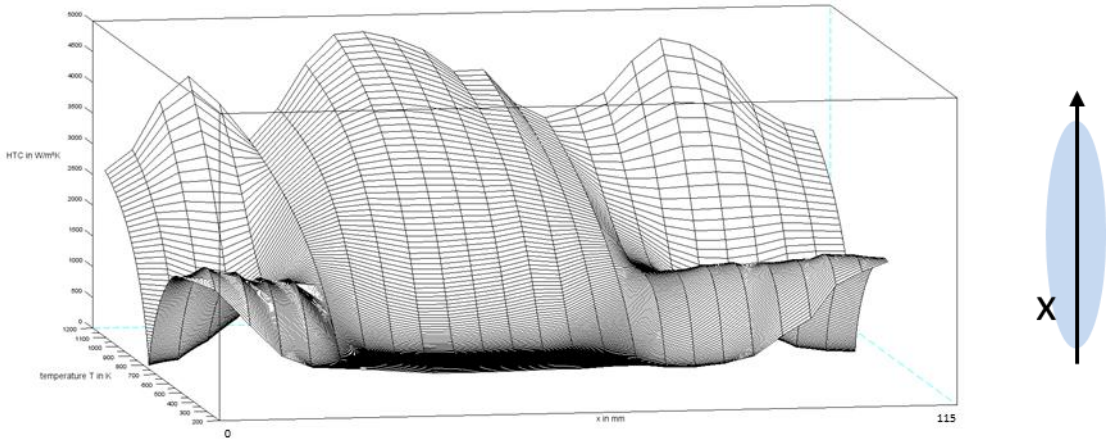

Figure 14 HTC-Temperature-Position profile of the large spreading, process parameter 175 l/h 5.6 bar

Figure 14 shows a temperature/position/HTC diagram along the large spreading side of the spray. The middle of the spray cone is represented by x = 57.5 mm. Figure 15 shows the temperature/position/HTC diagram along the small spray spreading. The middle of the spray is at x = 35 mm.

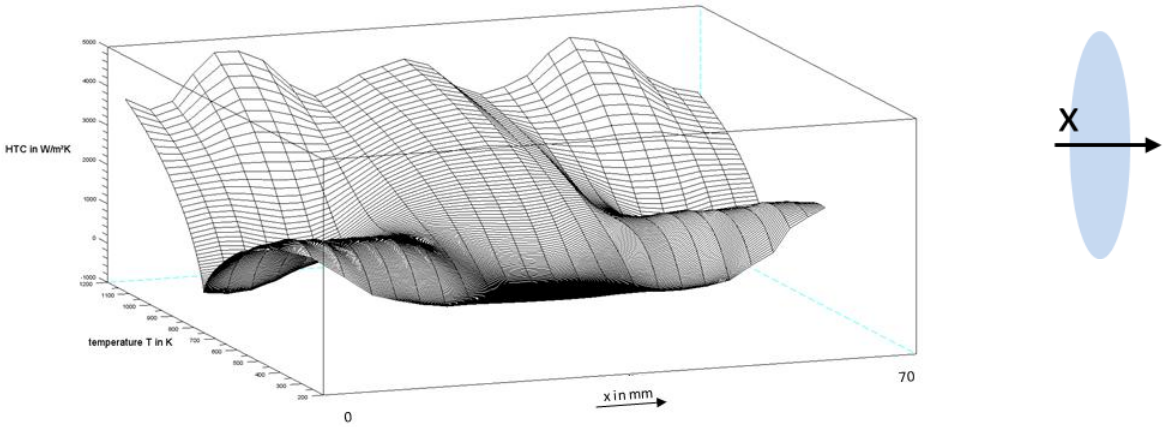

Figure 15 HTC-Temperature-Position profile of the small spreading, process parameter 175 l/h 5.6 bar

The measurements obtain high heat transfer coefficients at high temperatures in the middle of the spray and lower HTC towards the edge of the spray cone, similar to [3][11][12]. The large spreading has a higher HTC gradient at the border. The HTC-profile is based on the spray profile of the flow, impingement density and distribution. The high HTC peaks moves from high temperature to low temperature from the middle to the border. With lower temperature the HTC-profile flattens totally. This behaviour of the HTC-profile is based on the heat con-

duction in radial direction of the specimen. The thermal resistivity on the surface during spray cooling (HTC = α) and the thermal resistivity in the assay itself, depending on the heat conduction (λ) and the length (l), is almost at the same order of magnitude. The quotient between both resistivities represents the Biot number [15][16].

$$Bi = \frac{\alpha * l}{\lambda} \tag{5}$$

Heat transfer coefficients of 1500 W/m^{2}K up to 6000 W/m^{2}K during the cooling are at the same order of magnitude as the heat conduction of the assays. An average HTC of 3000 W/m^{2}K creates an average Biot number of Bi = 1 for the 5 mm specimen(for 6000 W/m^{2}K Bi = 2). The heat conduction in the assay is therefore almost at the same level. This effect is shown by the relatively high HTC at the spray border in figure 19 and figure 20. Although these areas are out of the direct spray impact area, high HTC of more than 4000 W/m^2 K are detected. These effects are not recognized by the second setup. The assay thickness creates much higher Biot number (Bi = 9, l = 45 mm, α = 3000 W/m^{2}K). The assay heat resistivity is much higher than the spray cooling heat resistivity. The main temperature gradient for the flexible spray field inside the assay and for the thermographic trial is not clearly defined between surface, length or radial direction of the assay.

These results are implemented into numerical simulations of specimen cooling behaviour. Therefor a simulation was performed with geometric and material data of the shouldered shaft specimen of figure 4. The cooling curves are compared from simulation and experimental trials. In figure 16 the comparison between the cooling curves present quite good agreements. Figure 17 represent the used simulation model. It is illustrated with local HTC distribution based on the results of the thermography measurement.

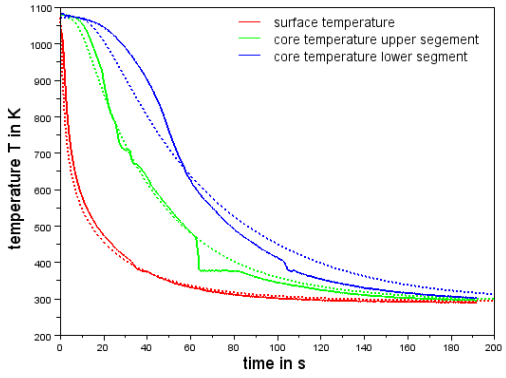

Figure 16 Comparison between simulated cooling curves and measured cooling curves

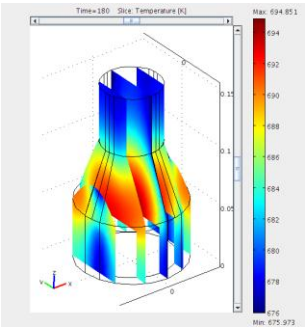

Figure 17 Simulation model with local HTCs.

Summary and Conclusions

The heat transfer during spray quenching with two phase flat cone spray nozzles is investigated. The used parameter range was a fluid volumetric flow rate of 0.25 l/h – 2.9 l/h and a gas pressure of 1 bar – 5.6 bar. The initial specimen temperature was about 1073 K and the detected surface temperature range reach from 1050 K - 400 K. Two experimental setups were used, the thermographic setup and a flexible spray field setup, as industrial used quenching setup. The measured HTC have peak values of more than 6000 W/m²K and depend on specimen surface temperature and position. The main parameter for the HTC distribution is the specimen surface temperature. The gas pressure influence to the cooling process is minimal. The fluid flow exhibits with an increasing flow a faster cooling reaction and a faster cooling of the specimen and therefor a higher HTC. Analysis of the cooling curves must select a wide range HTC function and low range HTC function. Low range HTC function exhibits the influence of the Leidenfrost effect. Wide range HTC function demonstrated the function of temperature and position to the HTC. The identified HTC and the distribution of the HTC in the impingement area are in agreement with previous investigations [3][11][12][18]. The temperature depending HTC distribution over the specimen surface includes also the not directly impingement faces, which shows the influence of the three dimensional heat conduction. These results are implemented into numerical cooling simulations.

For further investigations the complete three dimensional heat conduction terms will be implemented into the calculation of HTC during thermographic analysis. The heat transfer process during spray impingement on curved (her convex shaped) surfaces is to be investigated to describe the relevant HTC during spray quenching of specimen.

Acknowledgements

This work was supported by the BMWI (German Ministry of Economy and Technology) under the supervision of the AiF member society AWT (Arbeitsgemeinschaft Wärmebehandlung und Werkstofftechnik) in AiF project "Aluminium spray quenching" and the cooperative project "EcoForge". The work was performed as a cooperation of the University Bremen and the IWT Bremen, Germany.

References

[1] Petrus B., Zheng K., Zhou X., Brian G., Bentsman T., Bentsman J., Metallurgical and Materials Transactions B 42: 87-103 (2011)
[2] Sengupta J., Thomas B.G., Wells M.A., Metallurgical and Materials Transactions A 36: 187-204 (2005)
[3] Deiters T.A., Mudawar I., J. Heat Treat. 7: 9-18 (1989)
[4] Krause C., Gretzki T., Nürnberger F., Schapper M., Bach F.-W., Forsch Ingenieurwes 70: 237-242 (2006)
[5] Puschmann F., Specht E., Experimental Thermal and Fluid Science 28: 607-615 (2004)
[6] Rodman D., Kerber K., Yu Z., Mozgova I., Nürnberger F., Bach F.-W., Forsch Ingenieurwes.10. (2007)
[7] Schüttenberg S., Krause F., Hunkel M., Zoch H.-W., Fritsching U., Mat.-wiss. U. Werkstofftech. 40 (2009)
[8] Jungho K., Int. J. Of Heat and Fluid Flow 28: 753-767 (2007)
[9] Bernardin J.D., Mudawar I., Int. J. Heat Mass Transfer 40: 2579-2593 (1997)
[10] Hardin R.A., Liu' K., Kapoor A., Beckermann C., Metallurgical and Materials Transactions B 34: 297-306 (2003)
[11] Rodman D., Kerber K., Yu Z., Mozgova I., Nürnberger F., Bach F.-W., Forsch Ingenieurwes 75: 25-34 (2011)
[12] Krause C., Wulf E., Nürnberger F., Bach F.-W., Forsch Ingenieurwes 72: 163-173 (2008)
[13] Jescher R., Specht E., Köhler C., Theory and Technology of Quenching 73-92, Berlin: Springer (1992)
[14] Kang B.-S., Choi K.-J., KSME Int. J. 12: 734-740 (1998)
[15] Verein Deutscher Ingenieure, VDI Wärmeatlas, Ec, Berlin, Heidelberg: Springer (2006)
[16] Crowe C.T., Multiphase Flow Handbook, 3, London New York: Taylor&Francis (2006)
[17] Wendlestorf J., Spitzer K.-H., Wendlestorf R., Int. J. Heat Mass Transfer 51: 4902-4910, (2008)
[18] Mudawar I., Deiters T., Int. J. Heat Mass Transfer 37: 347-362, (2006)
[19] Puschmann F., Specht E., Schmidt J., Int. J. of Heat and Technology 19: 51-56 (2001)
[20] Tensi H., Liscic B., Luty W., Theory and Technology of Quenching, 4, Berlin: Springer (1992)
[21] Rodman D., Kerber K., Yu Z., Mozgova I., Nürnberger F., Bach F.-W., Forsch Ingenieurwes. 75: 25-34 (2007)